SUPPORTING INFORMATION TO:

In-vitro metabolites characterization of 1,3-diphenylguanidine and 1,3-di-o-tolylguanidine by high-resolution mass spectrometry and urinary profiling

Andrea Estévez-Danta [a,*], Iago Riveiro [a], María Lage-Díaz [a], José Benito Quintana [a], Rosa Montes[a], Rosario Rodil [a,*]

[a] Aquatic One Health Research Center (ARCUS) & Department of Analytical Chemistry, Nutrition and Food Chemistry. R. Constantino Candeira S/N, IIAA building, Universidade de Santiago de Compostela, 15782 Santiago de Compostela, Spain.

*Correspondence to: andreaestevez.danta@usc.es and rosario.rodil@usc.es

INDEX

Text S1. Analytical methodology for compound identification in urine

Instrumental analyses were carried out in an Agilent 1260 Infinity II LC equipped with a quaternary solvent pump, a thermostatted LC column compartment, and a sample manager. The U(H)PLC system was interfaced to an Agilent 6495 LC/QqQ triple quadrupole mass spectrometer. Chromatographic separation was performed under the same conditions as for the LC-QTOF methodology shown in Section 2.4 and the injection volume was set at 10 µL. To prevent system contamination, an InfinityLab PFC Delay Column (4.6 x 30mm) from Agilent was placed before the injector.

A Jet Stream electrospray ionization (ESI) source operating in positive mode was the interface between the LC system and the 6495 LC/QqQ triple quadrupole mass spectrometer at a fixed capillary and nozzle voltage of 2.5 and 0.5 kV, respectively. Nitrogen was used as sheath gas at 12 L min^{-1} and 400 °C and also as desolvation gas at 15 L min^{-1} and 215 °C.

Analyses were performed by MS/MS in selected reaction monitoring (SRM) mode using 166 V as fragmentor voltage. Table S1 summarizes the SRM transitions (Qn), ratios between the transitions, retention times (RT) and optimal collision energies (CE) for the target chemicals and the internal standard (Ib-d4). As no commercial standard of the metabolic products was available, the sample sets submitted to *in-vitro* metabolism, where metabolites were positive, were used to optimize the MS/MS parameters.

Table S1. Compound name, retention time (RT), transitions (*Q*n) used for quantification (*Q*1), and confirmation (*Q*2 and *Q*3), ratio between the transitions, optimal collision energy (CE) values for target chemicals and compound used as internal standards (IS).

Compound	RT (min)	Q_1 (*m/z*)	CE (eV)	Q_2 (*m/z*)	CE (eV)	Q_2/Q_1	Q_3 (*m/z*)	CE (eV)	Q_3/Q_1
DPG	10.1	212.0 -> 94.0	19	212.0 -> 119.0	25	1.1	212.0 -> 195.0	20	0.70
DPG-225	7.3	226.0 -> 108.0	19	226.0 -> 119.0	25	0.72	-	-	-
DPG-227	7.3	228.0 -> 135.0	25	228.0 -> 110.0	19	0.79	228.0 -> 211.0	19	0.42
DPG-387	6.0	388.0 -> 212.0	14	388.0 -> 270.0	15	0.27	-	-	-
DPG-403	6.2	404.0 -> 211.0	13	404.0 -> 212.0	13	1.3	404.0 -> 228.0	9	0.066
DTG	13.0	240.0 -> 133.0	17	240.0 -> 108.0	19	0.95	240.0 -> 223.0	25	0.45
DTG-253	14.1	254.0 -> 77.0	73	254.0 -> 106.0	44	0.18	254.0 -> 112.0	21	0.020
DTG-255	10.2	256.0 -> 124.0	25	256.0 -> 149.0	25	0.97	256.0 -> 221.0	21	0.40
DTG-415	9.5	416.0 -> 240.0	21	416.0 -> 284.0	19	0.30	-	-	-
DTG-431 (1)	6.5	432.0 -> 256.0	25	432.0 -> 149.0	44	0.12	432.0 -> 89.0	98	0.026
DTG-431 (2)	10.5	432.0 -> 256.0	25	432.0 -> 89.0	98	0.13	432.0 -> 149.0	44	0.030
Ib-d4	18.4	433.0 -> 211.0	24	433.0 -> 195.0	24	0.28	-	-	-

Table S2. Suspect list for DPG

Name	Chemical Formulae	Monoisotopic Mass	Source [a]
DPG	$C_{13}H_{13}N_3$	211.1109	-
DPG-135	$C_7H_9N_3$	135.0796	QSAR
DPG-93	C_6H_7N	93.0578	QSAR
DPG-269	$C_{12}H_{15}NO_6$	269.0899	Self-proposal
DPG-173	$C_6H_7NO_3S$	173.0147	Self-proposal
DPG-311	$C_{13}H_{17}N_3O_6$	311.1117	Self-proposal
DPG-215	$C_7H_9N_3O_3S$	215.0365	Self-proposal
DPG-227	$C_{13}H_{13}N_3O$	227.1059	Sieira et al., 2020 / Clement et al., 1993
DPG-387	$C_{19}H_{21}O_6N_3$	387.1430	GloryX
DPG-291	$C_{13}H_{13}N_3O_3S$	291.0678	Self-proposal
DPG-212	$C_{13}H_{12}N_2O$	212.0950	QSAR
DPG-228	$C_{13}H_{12}N_2O_2$	228.0899	QSAR
DPG-244	$C_{13}H_{12}N_2O_3$	244.0848	Self-proposal
DPG-243	$C_{13}H_{13}N_3O_2$	243.1008	Biotransformer
DPG-136	$C_7H_8N_2O$	136.0637	QSAR
DPG-312	$C_{13}H_{16}N_2O_7$	312.0958	Self-proposal
DPG-232	$C_7H_8N_2SO_5$	232.0154	Self-proposal
DPG-209	$C_{13}H_{11}N_3$	209.0953	Self-proposal
DPG-225	$C_{13}H_{11}N_3O$	225.0902	Sieira et al., 2020
DPG-241	$C_{13}H_{11}N_3O_2$	241.0851	Self-proposal
DPG-403	$C_{19}H_{21}N_3O_7$	403.1380	QSAR
DPG-401	$C_{19}H_{19}N_3O_7$	401.1223	Self-proposal
DPG-305	$C_{13}H_{11}N_3O_4S$	305.0470	Self-proposal
DPG-289	$C_{13}H_{11}N_3O_3S$	289.0521	Self-proposal
DPG-243	$C_{13}H_{13}N_3O_2$	243.1008	Sieira et al., 2020
DPG-259	$C_{13}H_{13}N_3O_3$	259.0957	Biotransformer
DPG-247	$C_{12}H_{13}N_3O_3$	247.0957	Self-proposal

*Sieira BJ, Montes R, Touffet A, Rodil R, Cela R, Gallard H, et al. Chlorination and bromination of 1,3-diphenylguanidine and 1,3-di-o-tolylguanidine: Kinetics, transformation products and toxicity assessment. Journal of Hazardous Materials 2020; 385: 121590.
*B. Clement, T. Kunze, In vitro oxygenation of N,N'-diphenylguanidines, Xenobiotica, 23 (1993) 155-167.
*QSAR Toolbox. "QSAR Toolbox webpage." Retrieved October 2023, from https://qsartoolbox.org/.
*GLORYx Predicting Phase I and Phase II Metabolites. Stork C, Embruch G, Šícho M, de Bruyn Kops C, Chen Y, Svozil D, et al. NERDD: a web portal providing access to in silico tools for drug discovery. *Bioinformatics 2019; 36: 1291-1292
Biotranformer. "Biotranformer 3.0 webpage." Retrieved October 2023, from https://biotransformer.ca/.

Table S3. Suspect list for DTG

Name	Chemical Formulae	Monoisotopic Mass	Source [a]
DTG	$C_{15}H_{17}N_3$	239.1422	-
DTG-149	$C_8H_{11}N_3$	149.0953	Sieira et al., 2020
DTG-165	$C_8H_{11}N_3O$	165.0902	Self-proposal
DTG-163	$C_8H_9N_3O$	163.0746	Self-proposal
DTG-179	$C_8H_9N_3O_2$	179.0695	Self-proposal
DTG-107	C_7H_9N	107.0735	QSAR
DTG-123	C_7H_9NO	123.0684	Self-proposal
DTG-121	C_7H_7NO	121.0528	Self-proposal
DTG-137	$C_7H_7NO_2$	137.0477	Self-proposal
DTG-283	$C_{13}H_{17}NO_6$	283.1056	Self-proposal
DTG-187	$C_7H_9NO_3S$	187.0303	Self-proposal
DTG-325	$C_{14}H_{19}N_3O_6$	325.1274	Self-proposal
DTG-229	$C_8H_{11}N_3O_3S$	229.0521	Self-proposal
DTG-255	$C_{15}H_{17}N_3O$	255.1371	Sieira et al., 2020
DTG-415	$C_{21}H_{25}O_6N_3$	415.1743	GloryX
DTG-319	$C_{15}H_{17}N_3O_3S$	319.0991	Self-proposal
DTG-253	$C_{15}H_{15}N_3O$	253.1215	QSAR
DTG-269	$C_{15}H_{15}N_3O_2$	269.1164	GloryX
DTG-240	$C_{15}H_{16}N_2OS$	240.1263	QSAR
DTG-256	$C_{15}H_{16}N_2O_2$	256.1212	QSAR
DTF-254	$C_{15}H_{14}N_2O_2$	254.1055	QSAR
DTG-270	$C_{15}H_{14}N_2O_3$	270.1004	QSAR
DTG-272	$C_{15}H_{16}N_2O_3$	272.1161	Self-proposal
DTG-286	$C_{15}H_{14}N_2O_4$	286.0954	Self-proposal
DTG-300	$C_{15}H_{12}N_2O_5$	300.0746	Self-proposal
DTG-271	$C_{15}H_{17}N_3O_2$	271.1321	QSAR
DTG-269	$C_{15}H_{15}N_3O_2$	269.1164	QSAR
DTG-285	$C_{15}H_{15}N_3O_3$	285.1113	Self-proposal
DTG-267	$C_{15}H_{13}N_3O_2$	267.1008	Self-proposal
DTG-299	$C_{15}H_{13}N_3O_4$	299.0906	Self-proposal
DTG-150	$C_8H_{10}N_2O$	150.0793	QSAR
DTG-166	$C_8H_{10}N_2O_2$	166.0742	Self-proposal
DTG-180	$C_8H_8N_2O_3$	180.0535	Self-proposal
DTG-196	$C_8H_8N_2O_4$	196.0484	Self-proposal
DTG-342	$C_{14}H_{18}N_2O_8$	342.1063	Self-proposal
DTG-246	$C_8H_{10}N_2SO_5$	246.0310	Self-proposal
DTG-237	$C_{15}H_{15}N_3$	237.1266	Sieira et al., 2020
DTG-253	$C_{15}H_{15}N_3O$	253.1215	Sieira et al., 2020
DTG-269	$C_{15}H_{15}N_3O_2$	269.1164	Self-proposal
DTG-283	$C_{15}H_{13}N_3O_3$	283.0957	Self-proposal
DTG-267	$C_{15}H_{13}N_3O_2$	267.1008	Self-proposal
DTG-431	$C_{21}H_{25}N_3O_7$	431.1693	Self-proposal
DTG-271	$C_{15}H_{17}N_3O_2$	271.1321	Self-proposal
DTG-431	$C_{21}H_{25}N_3O_7$	431.1693	Self-proposal
DTG-447	$C_{21}H_{25}N_3O_8$	447.1642	Self-proposal
DTG-312	$C_{15}H_{17}N_3O_3$	312.0958	Biotransformer

[*] Sieira BJ, Montes R, Touffet A, Rodil R, Cela R, Gallard H, et al. Chlorination and bromination of 1,3-diphenylguanidine and 1,3-di-o-tolylguanidine: Kinetics, transformation products and toxicity assessment. Journal of Hazardous Materials 2020; 385: 121590.

*QSAR Toolbox. "QSAR Toolbox webpage." Retrieved October 2023, from https://qsartoolbox.org/.

*GLORYx Predicting Phase I and Phase II Metabolites. Stork C, Embruch G, Šícho M, de Bruyn Kops C, Chen Y, Svozil D, et al. NERDD: a web portal providing access to in silico tools for drug discovery. Bioinformatics 2019; 36: 1291-1292

*Biotranformer. "Biotranformer 3.0 webpage." Retrieved October 2023, from https://biotransformer

Figure S1. Overview of quality controls employed during the Phase I in-vitro human liver metabolism assay

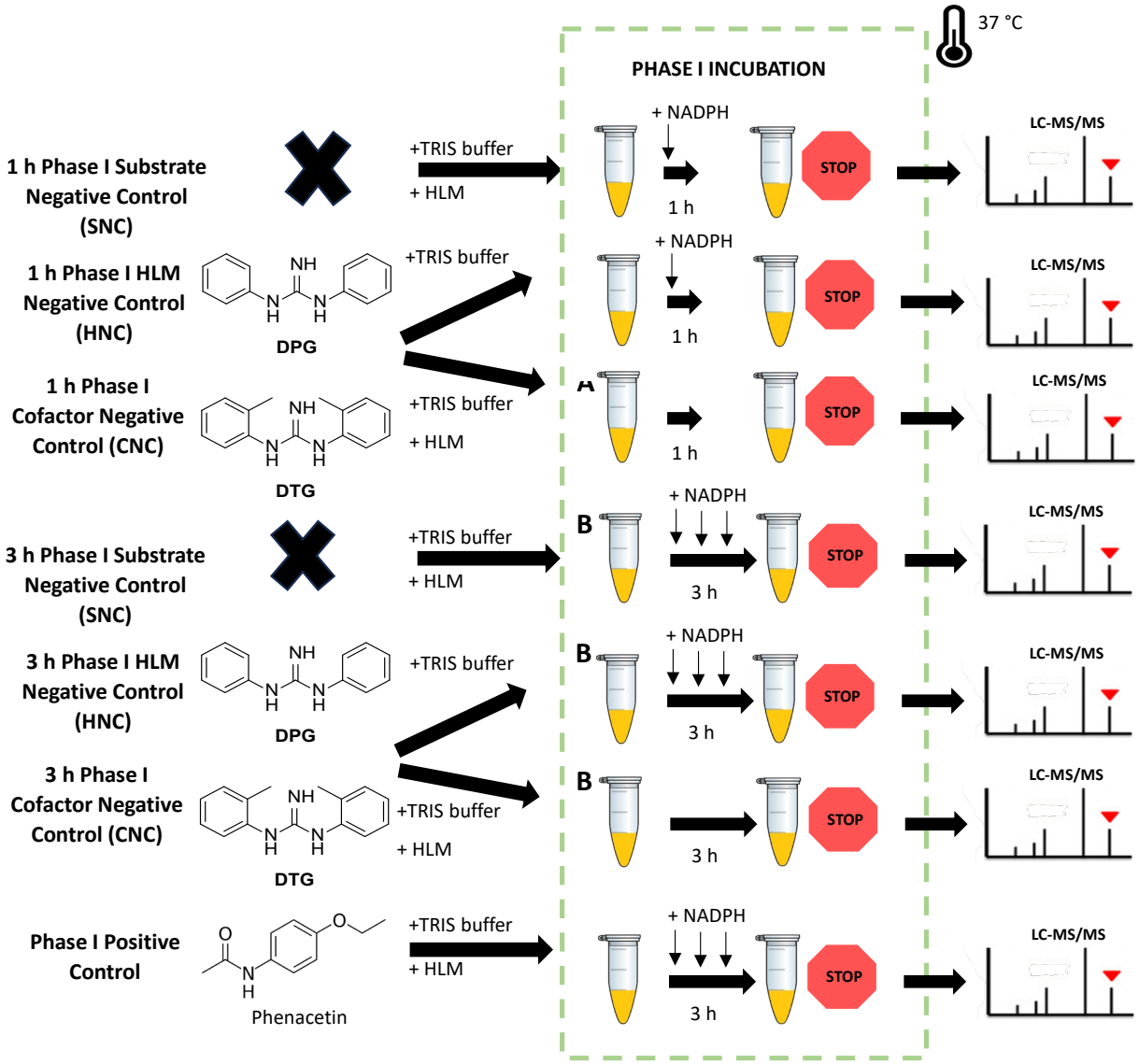

Figure S2. Overview of quality controls employed during the Phase II in-vitro human liver metabolism assay

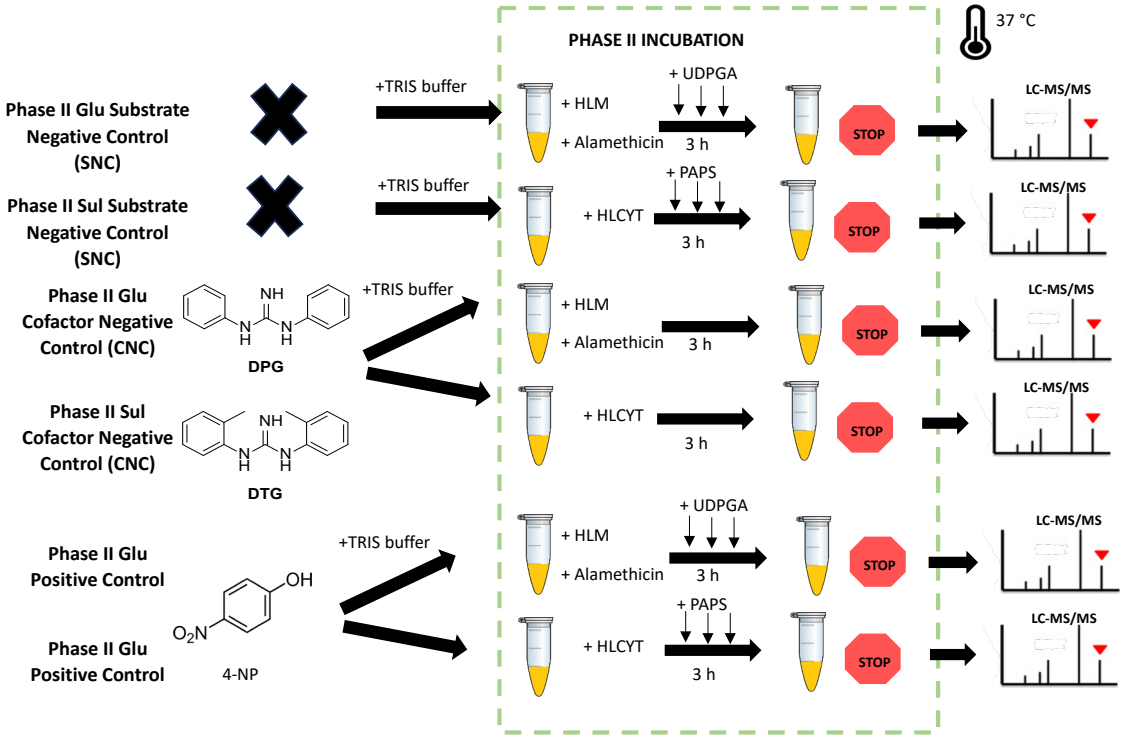

Figure S3. Extracted ion chromatogram, molecular structure and MS/MS spectrum at 20 V in positive mode of (a) phenacetin, (b) P-M1 and (c) P-M2

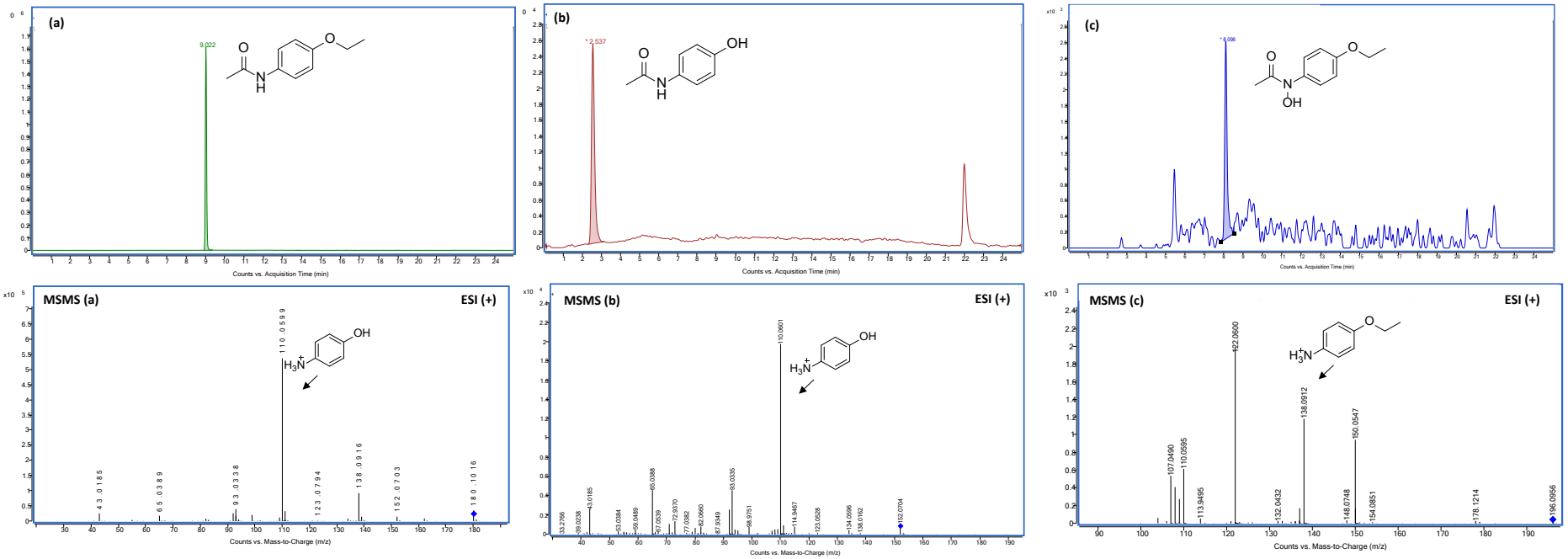

References:

[1] J. A. Hinson, Environ Health Perspect 1983 Vol. 49 Pages 71-9, Accession Number: 6339229 PMCID: PMC1569121 DOI: 10.1289/ehp.834971

[2] C. Christia, K. M. da Silva, G. Poma, A. L. N. van Nuijs and A. Covaci Toxicology Letters 2022 Vol. 356 Pages 33-40 DOI: https://doi.org/10.1016/j.toxlet.2021.12.005

Figure S4. Extracted ion chromatogram, molecular structure and MS/MS spectrum at 20 V of (a) 4-nitrophenol, (b) 4NP-G and (c) 4NP-S.

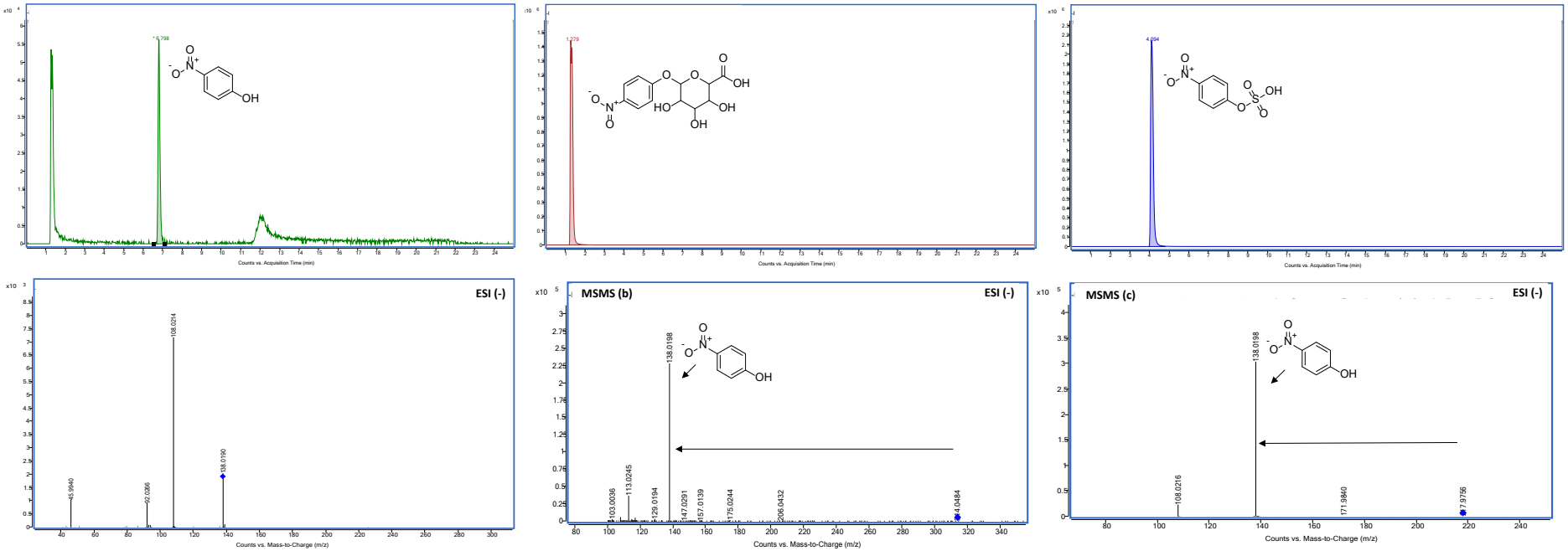

References

[1] R. H. Tukey and C. P. Strassburg , Annu Rev Pharmacol Toxicol 2000 Vol. 40 Pages 581-616 Accession Number: 10836148 DOI: 10.1146/annurev.pharmtox.40.1.581

[2] N. Gamage, A. Barnett, N. Hempel, R. G. Duggleby, K. F. Windmill, J. L. Martin, et al. Toxicological Sciences 2006 Vol. 90 Issue 1 Pages 5-22 DOI: 10.1093/toxsci/kfj061

Figure S5. Volcano plots of *m/z* values measured in ESI (+) and ESI (-) modes in Phase I samples for DPG. Features statistically significant are represented in green color (p-value < 0.05 and a log10 FC > 1).

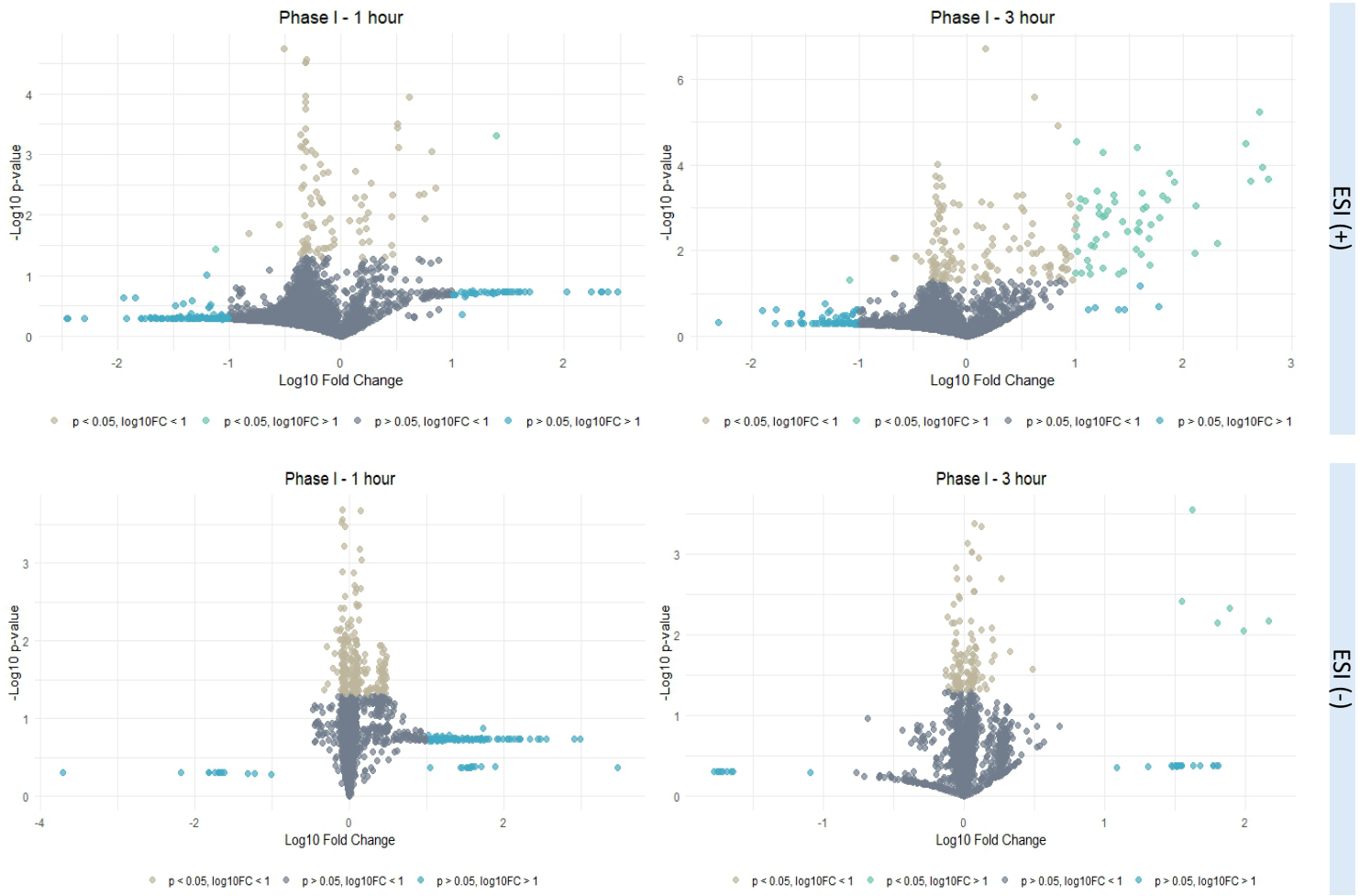

Figure S6. Volcano plots of *m/z* values measured in ESI (+) and ESI (-) modes in Phase I samples for DTG. Features statistically significant are represented in green color (p-value < 0.05 and a log10 FC > 1).

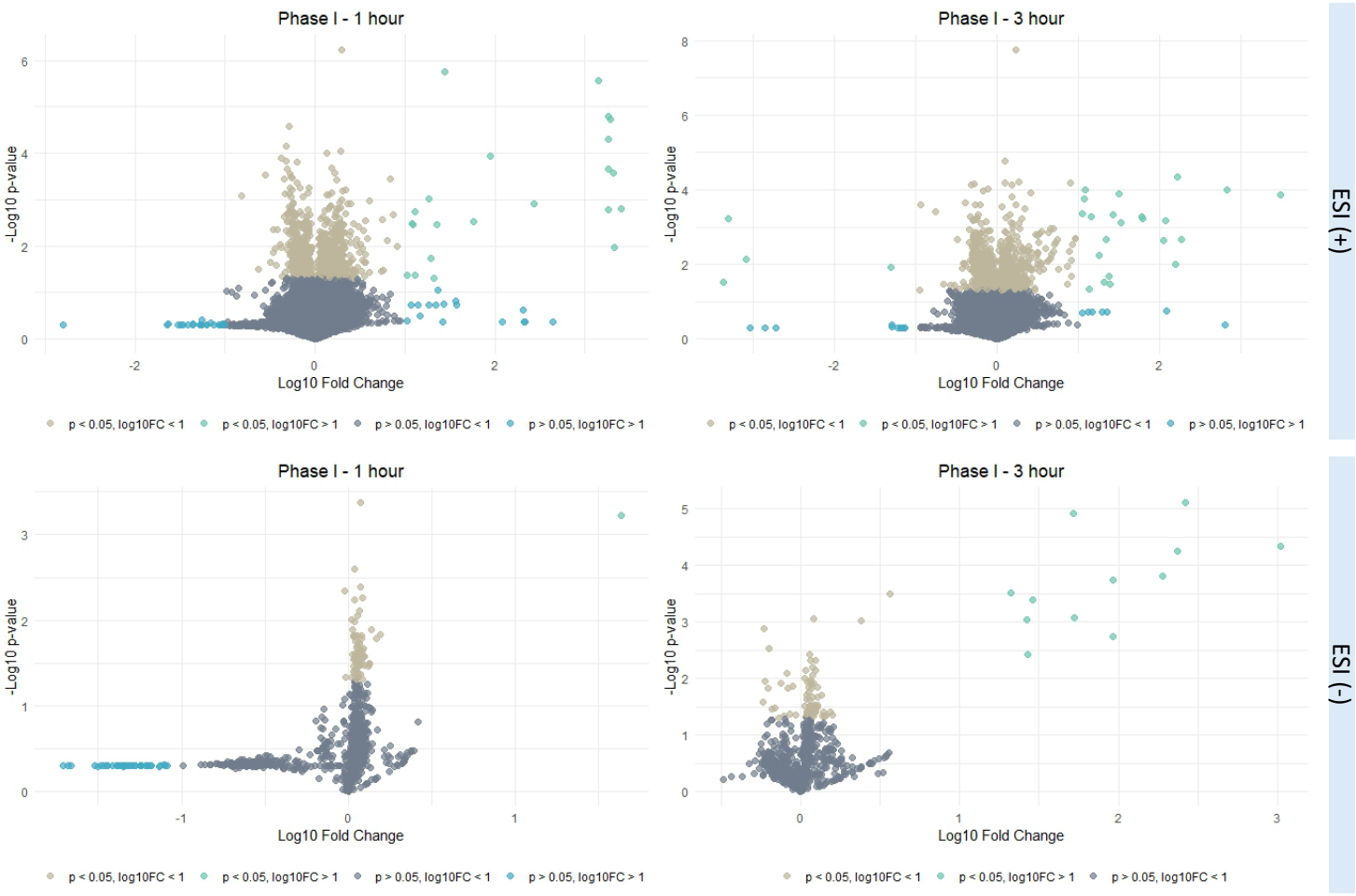

Figure S7. Volcano plots of *m/z* values measured in ESI (+) and ESI (-) modes in Phase II samples for DPG. Features statistically significant are represented in green color (p-value < 0.05 and a log10 FC > 1).

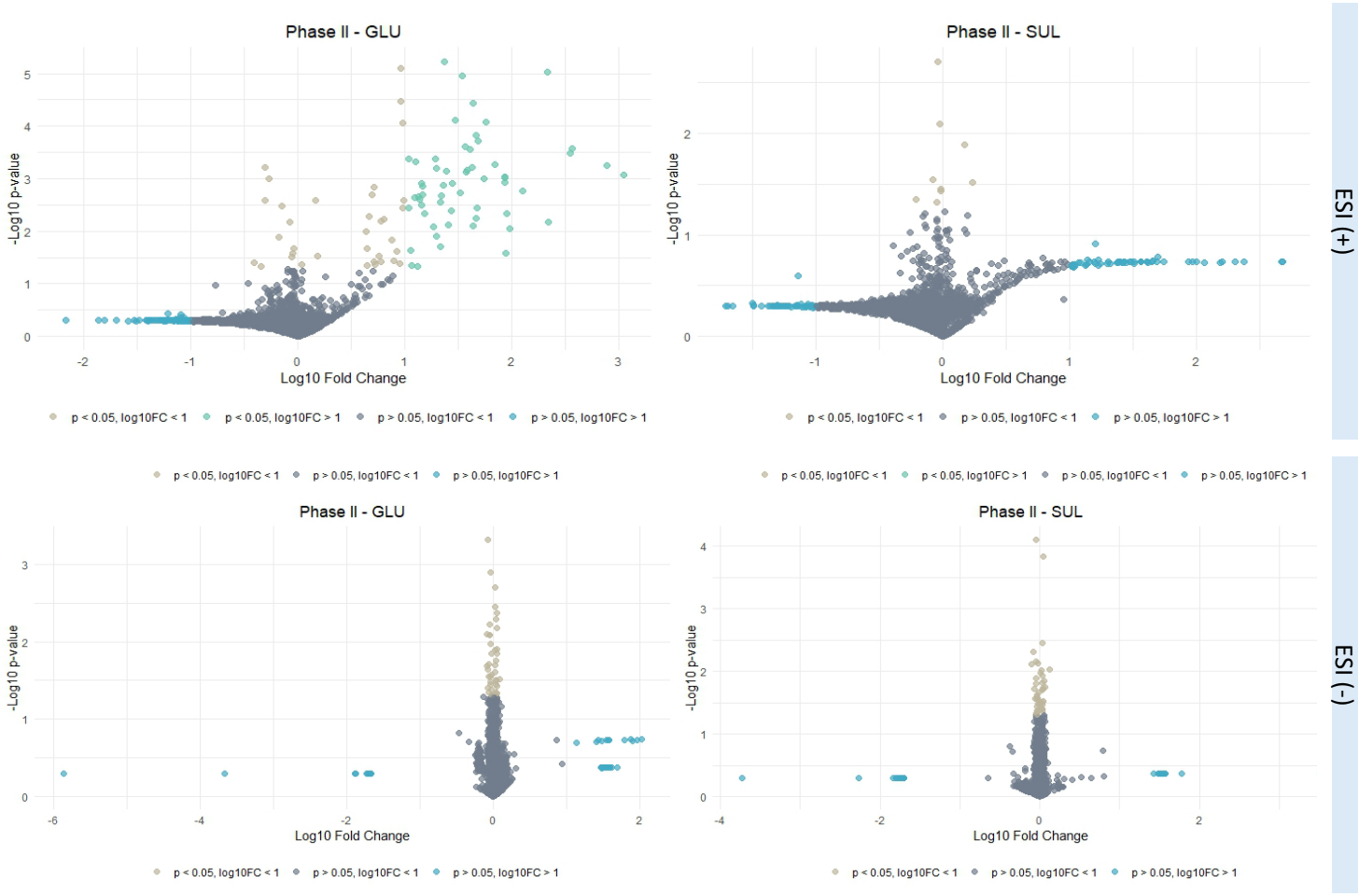

Figure S8. Volcano plots of *m/z* values measured in ESI (+) and ESI (-) modes in Phase II samples for DTG. Features statistically significant are represented in green color (p-value < 0.05 and a log10 FC > 1).

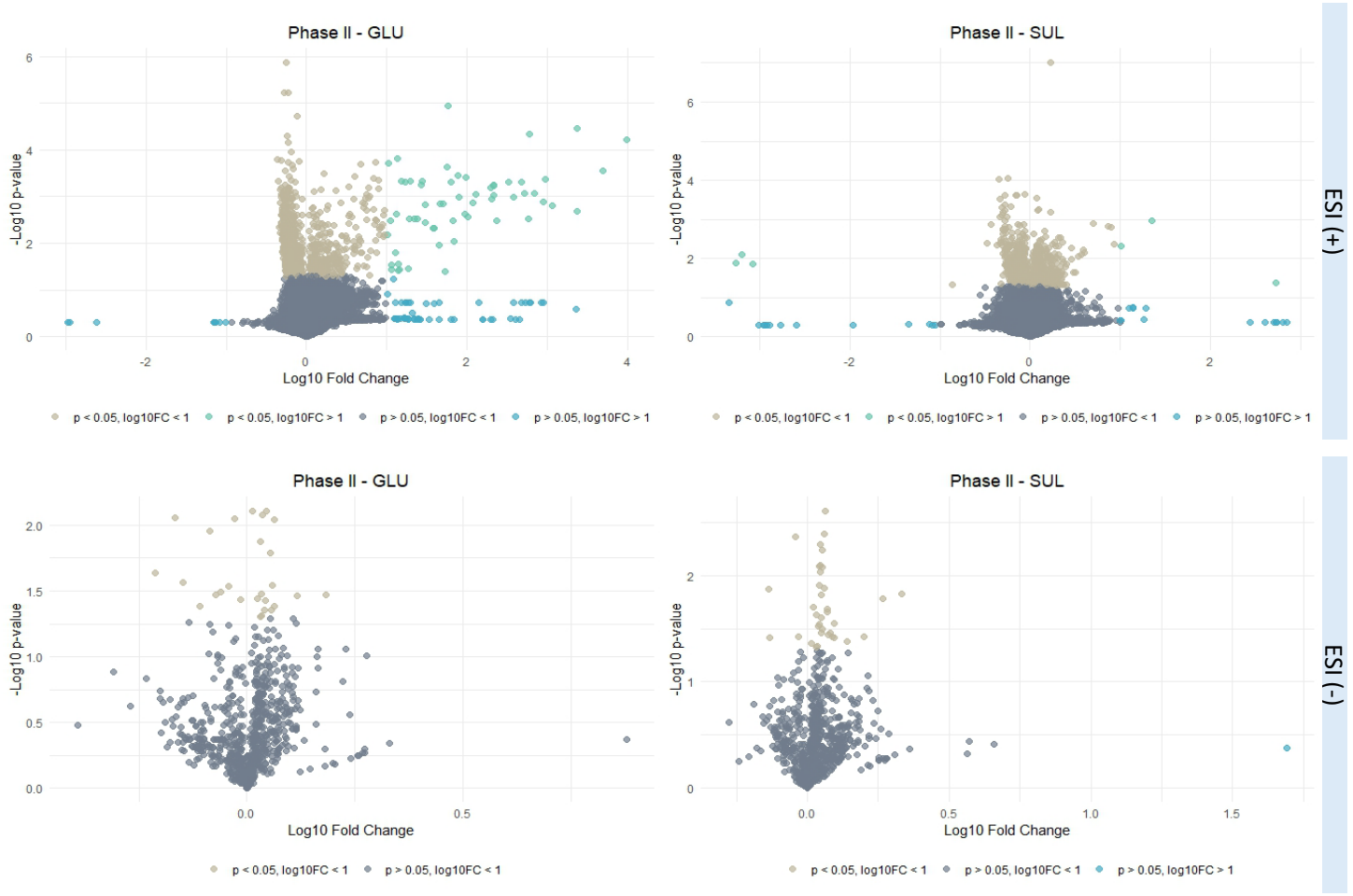

Figure S9. Extracted ion chromatogram (a) MS/MS spectrum at 20 V in positive (b) and negative mode (c) and fragmentation pathway (d) of DPG.

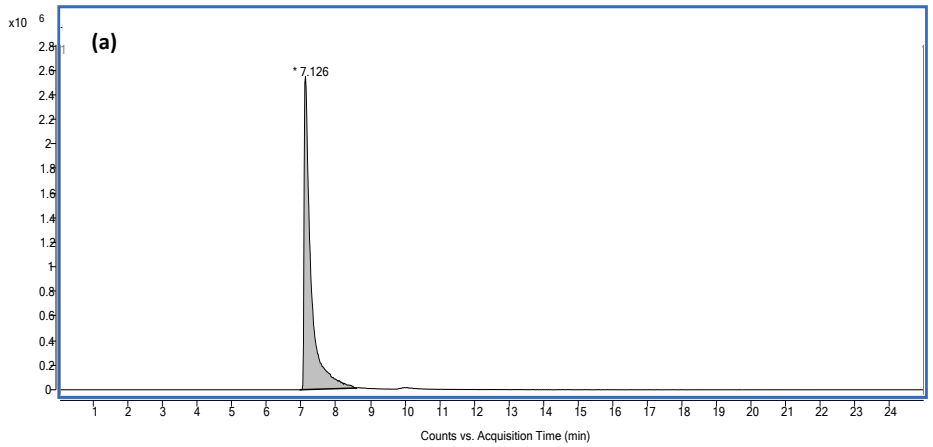

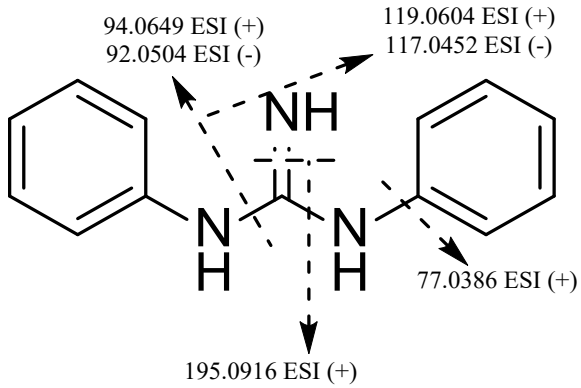

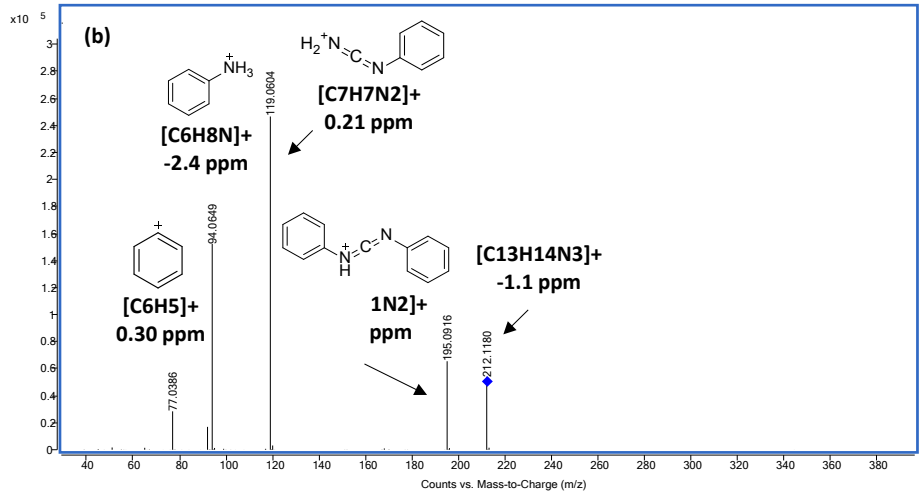

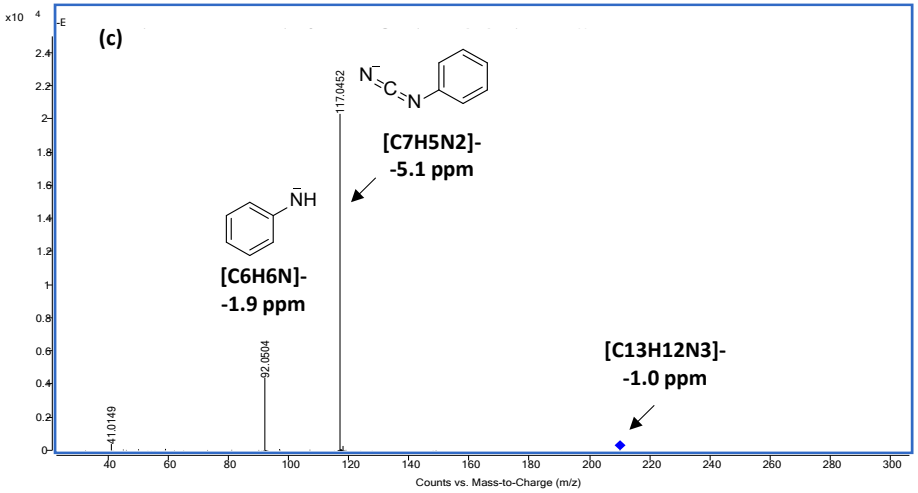

Figure S10. Extracted ion chromatogram (a), MS/MS spectrum at 20 V in positive (b) and negative mode (c) and fragmentation pathway (d) of DTG.

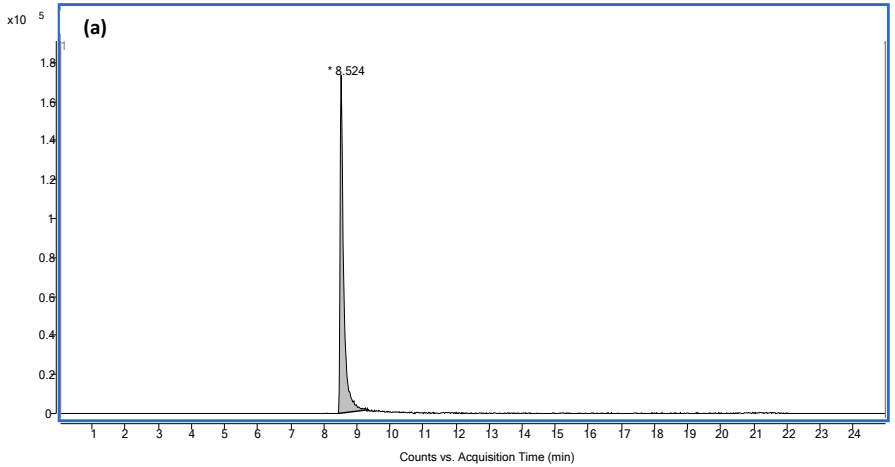

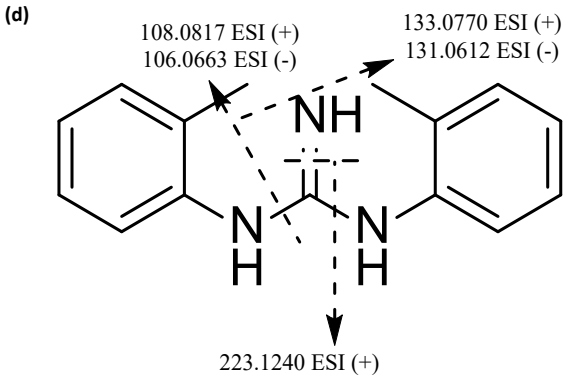

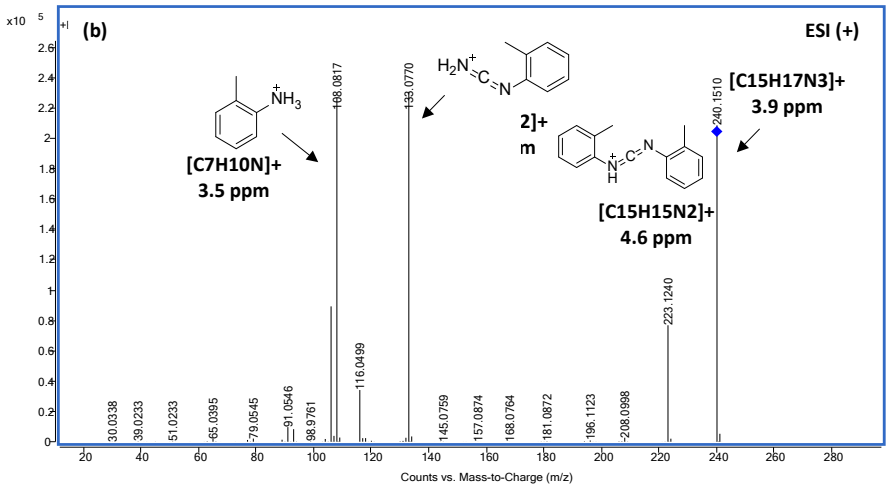

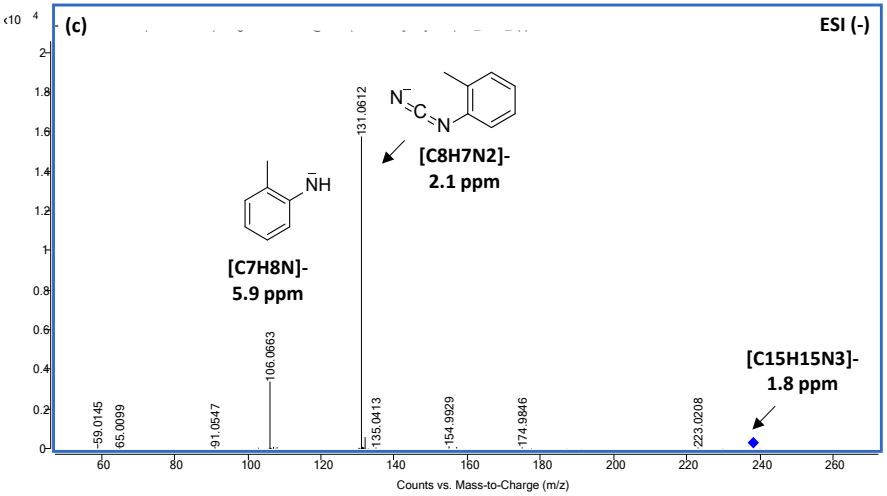

Figure S11.a Extracted ion chromatogram and MS/MS spectrum at 20 V with proposed fragmentation pattern for DPG-225.

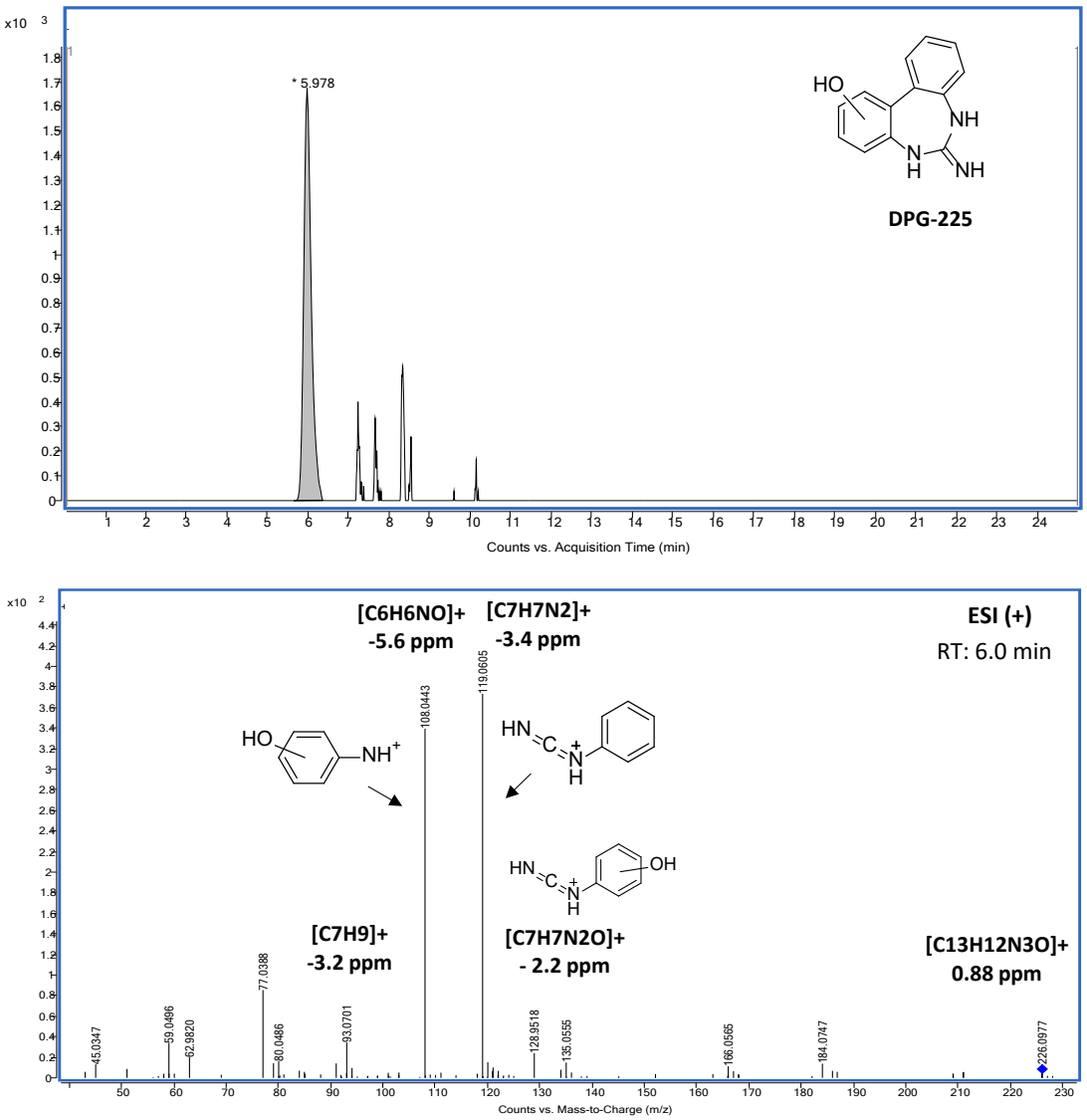

Figure S11.b Extracted ion chromatogram and MS/MS spectrum at 20 V with proposed fragmentation pattern for DPG-227.

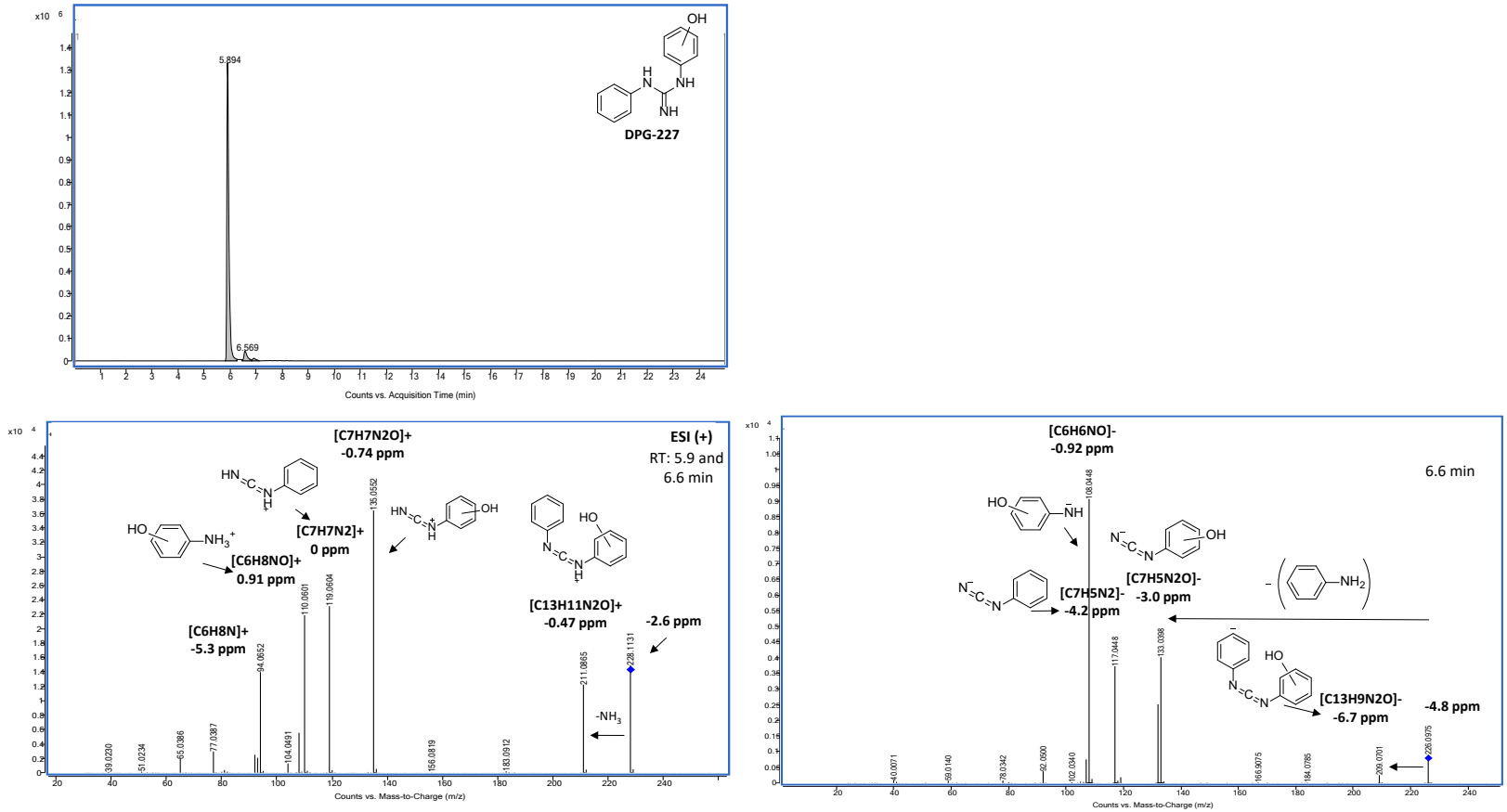

Figure S11.c Extracted ion chromatogram and MS/MS spectrum at 20 V with proposed fragmentation pattern for DPG-228.

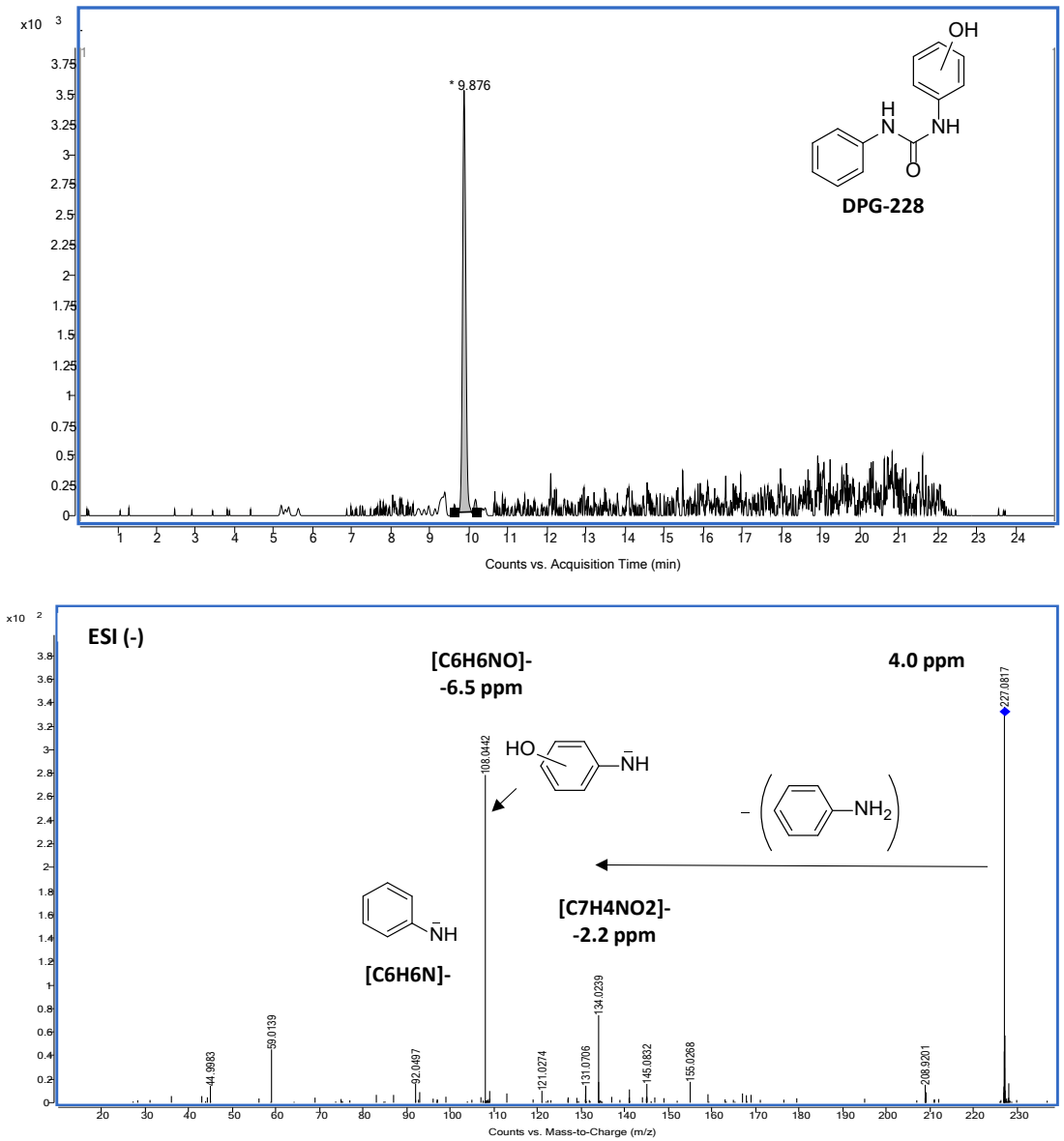

Figure S11.d Extracted ion chromatogram and MS/MS spectrum at 20 V with proposed fragmentation pattern for DPG-243.

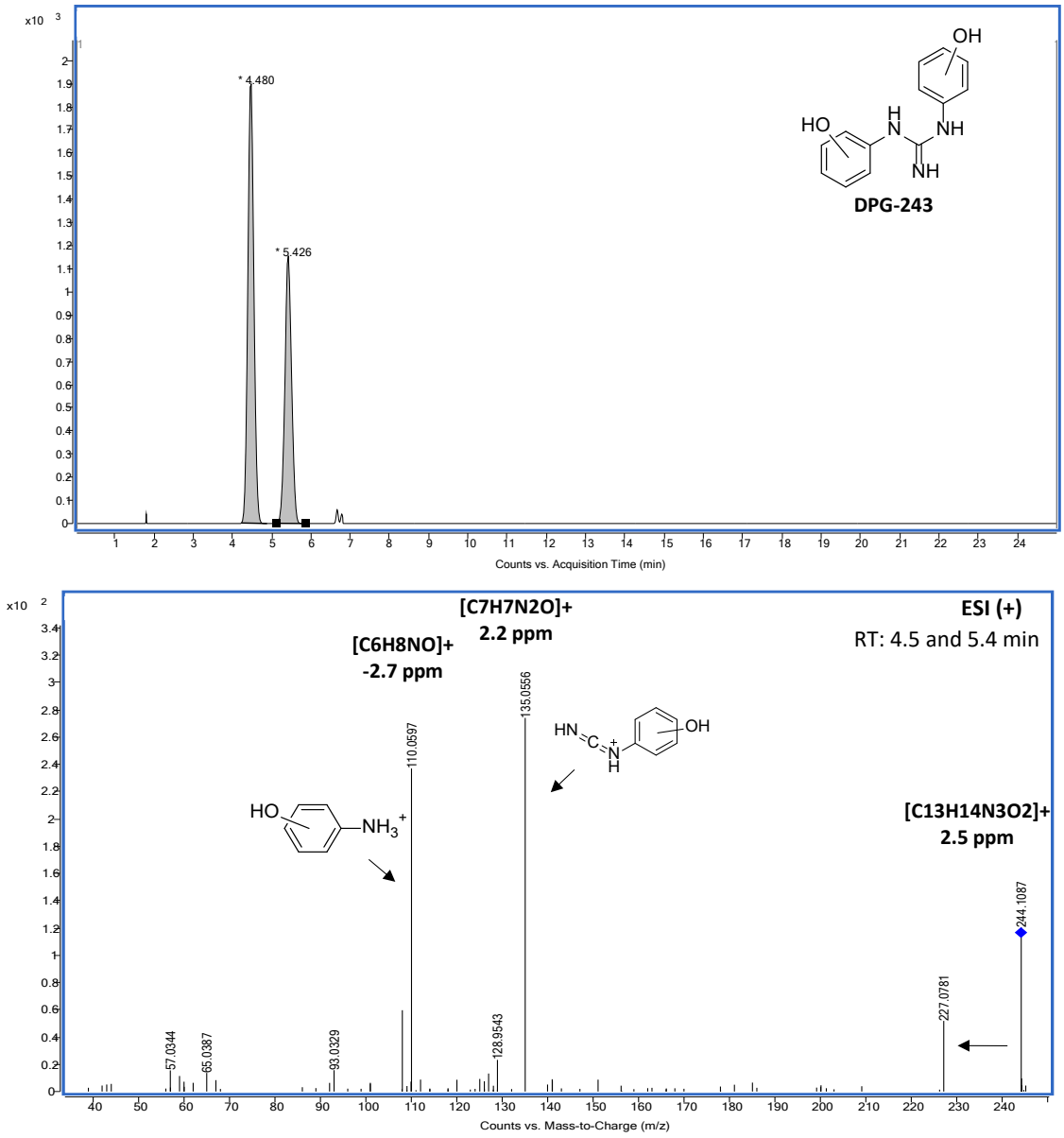

Figure S12.a Extracted ion chromatogram and MS/MS spectrum at 20 V with proposed fragmentation pattern for DTG-253.

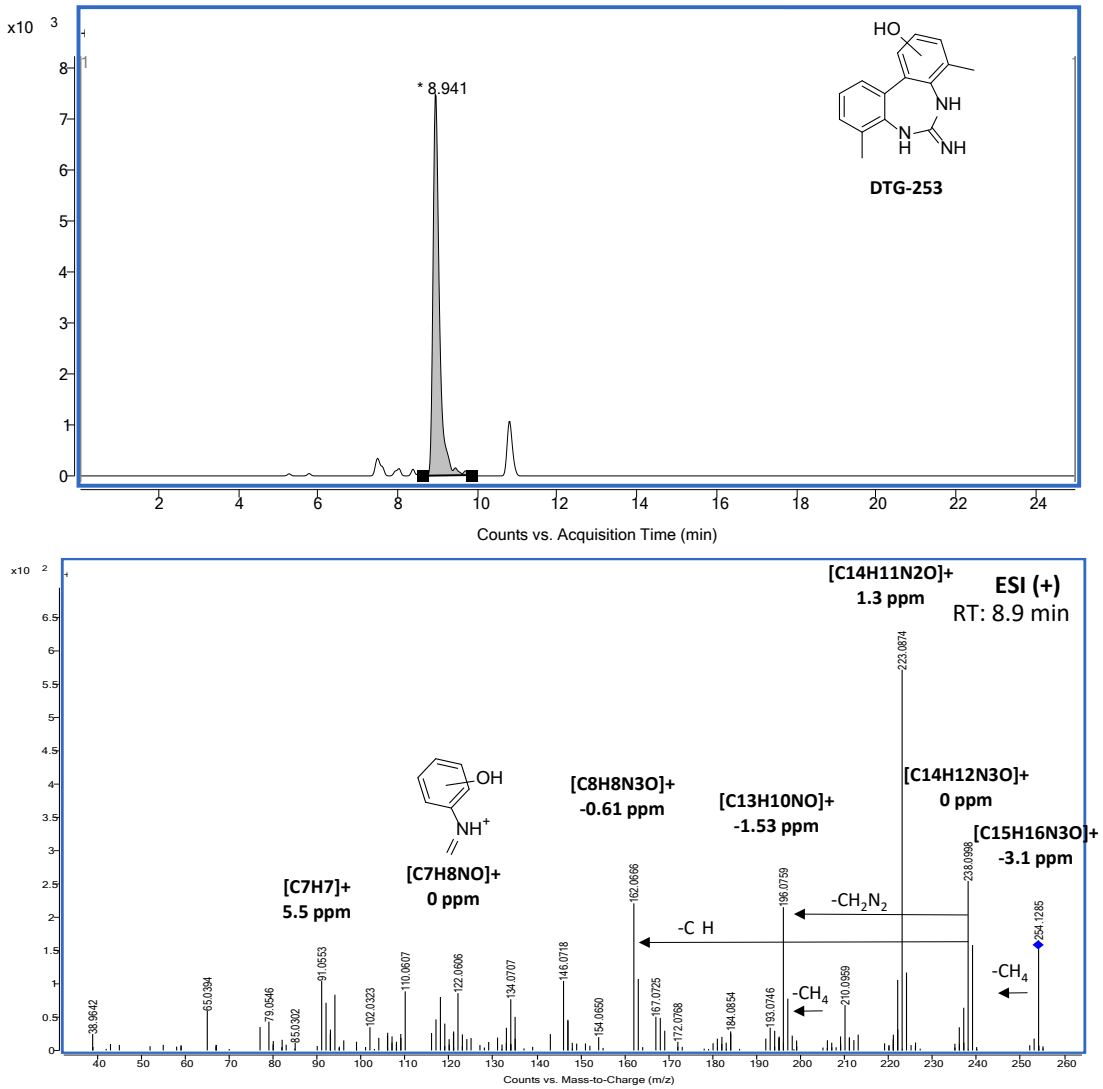

Figure S12.b Extracted ion chromatogram and MS/MS spectrum at 20 V with proposed fragmentation pattern for DTG-256.

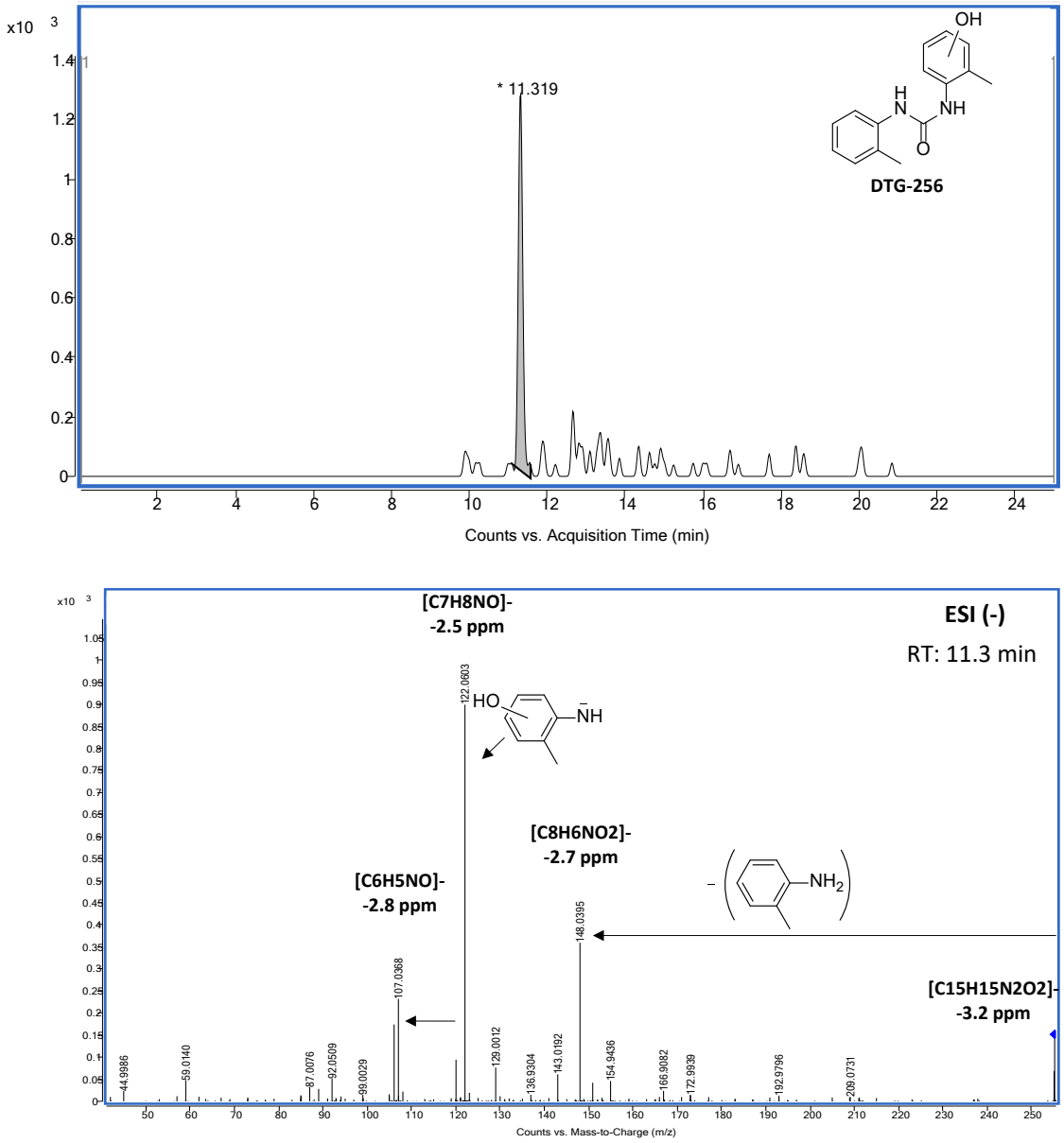

Figure S12.c Extracted ion chromatogram and MS/MS spectrum at 20 V with proposed fragmentation pattern for DTG-271.

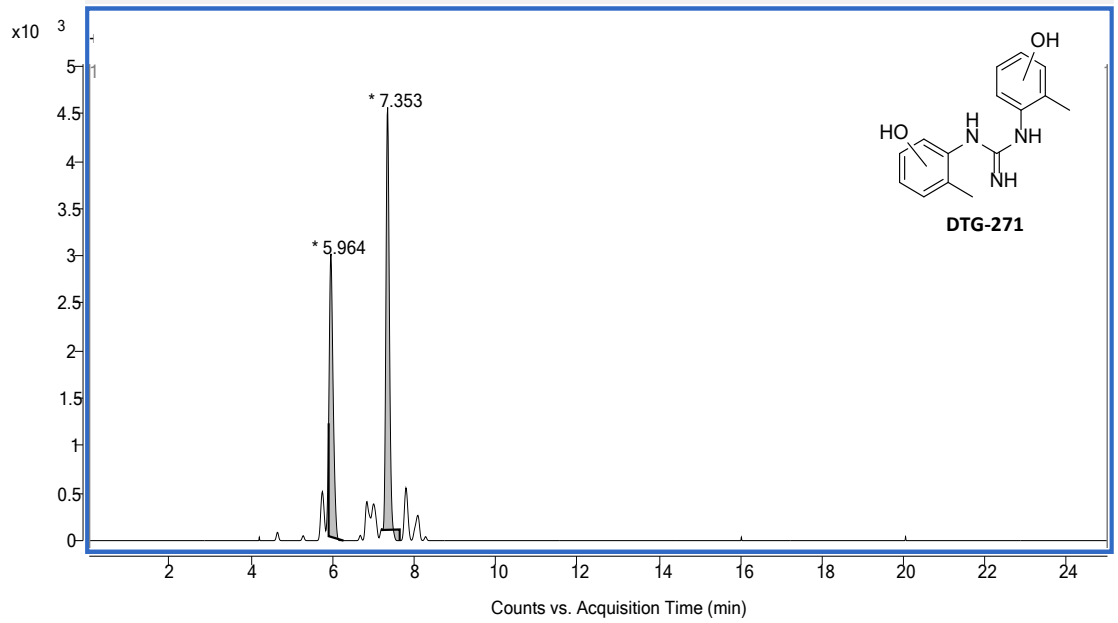

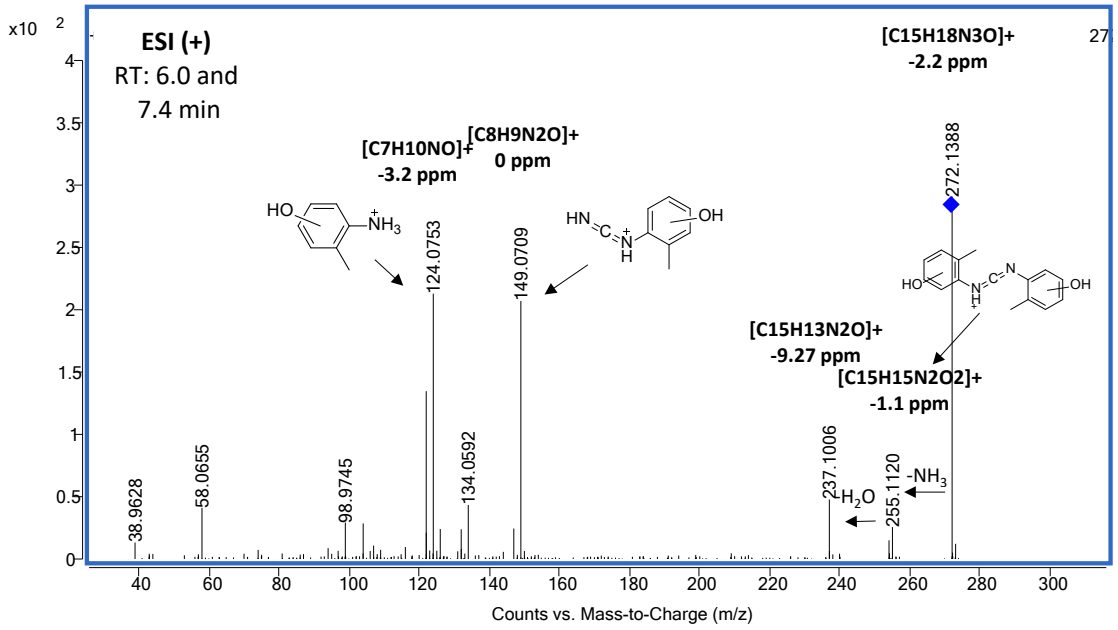

Figure S13.a Extracted ion chromatogram and MS/MS spectrum at 20 V with proposed fragmentation pattern for DPG-387.

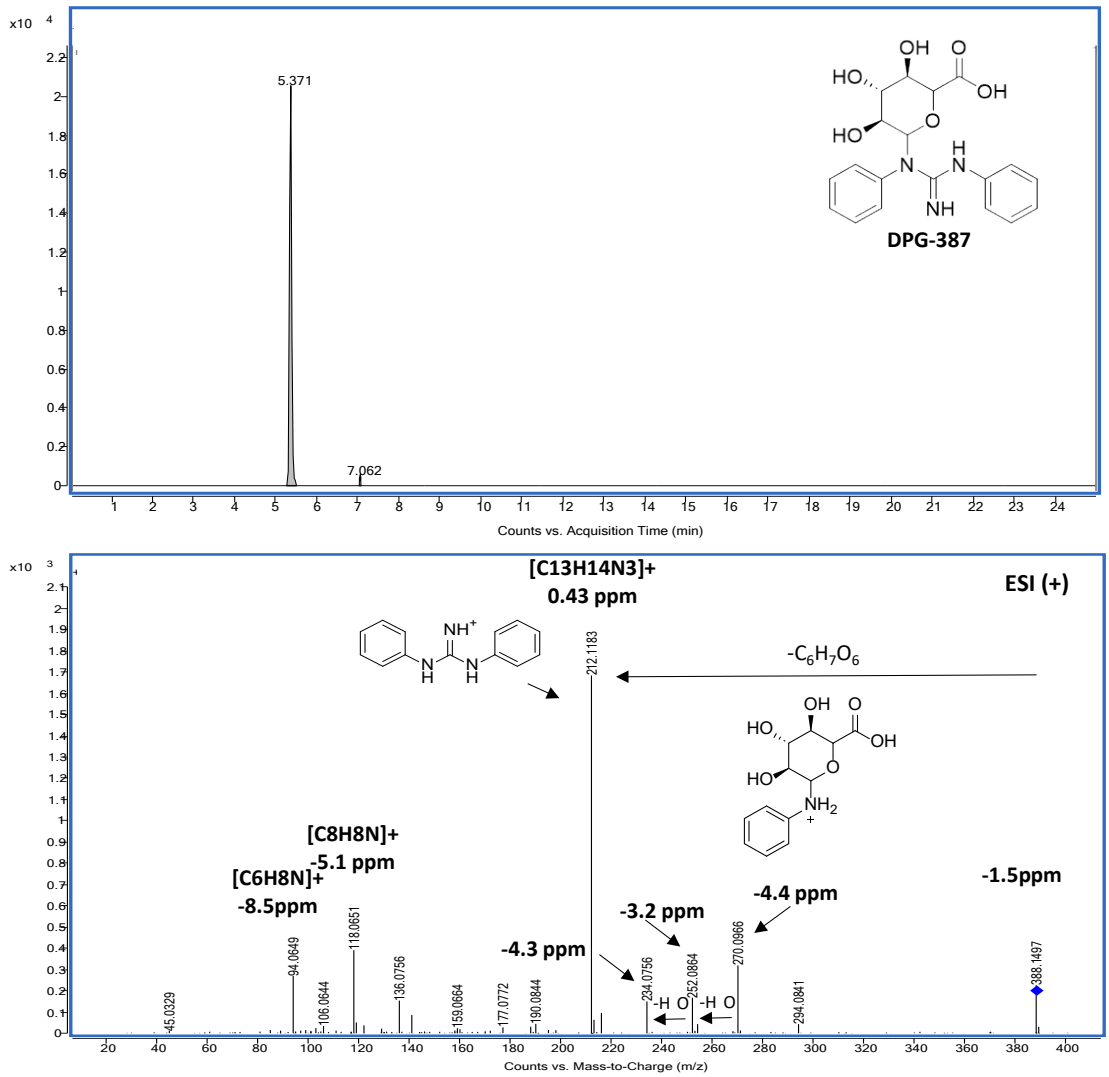

Figure S13.b Extracted ion chromatogram and MS/MS spectrum at 20 V with proposed fragmentation pattern for DPG-403.

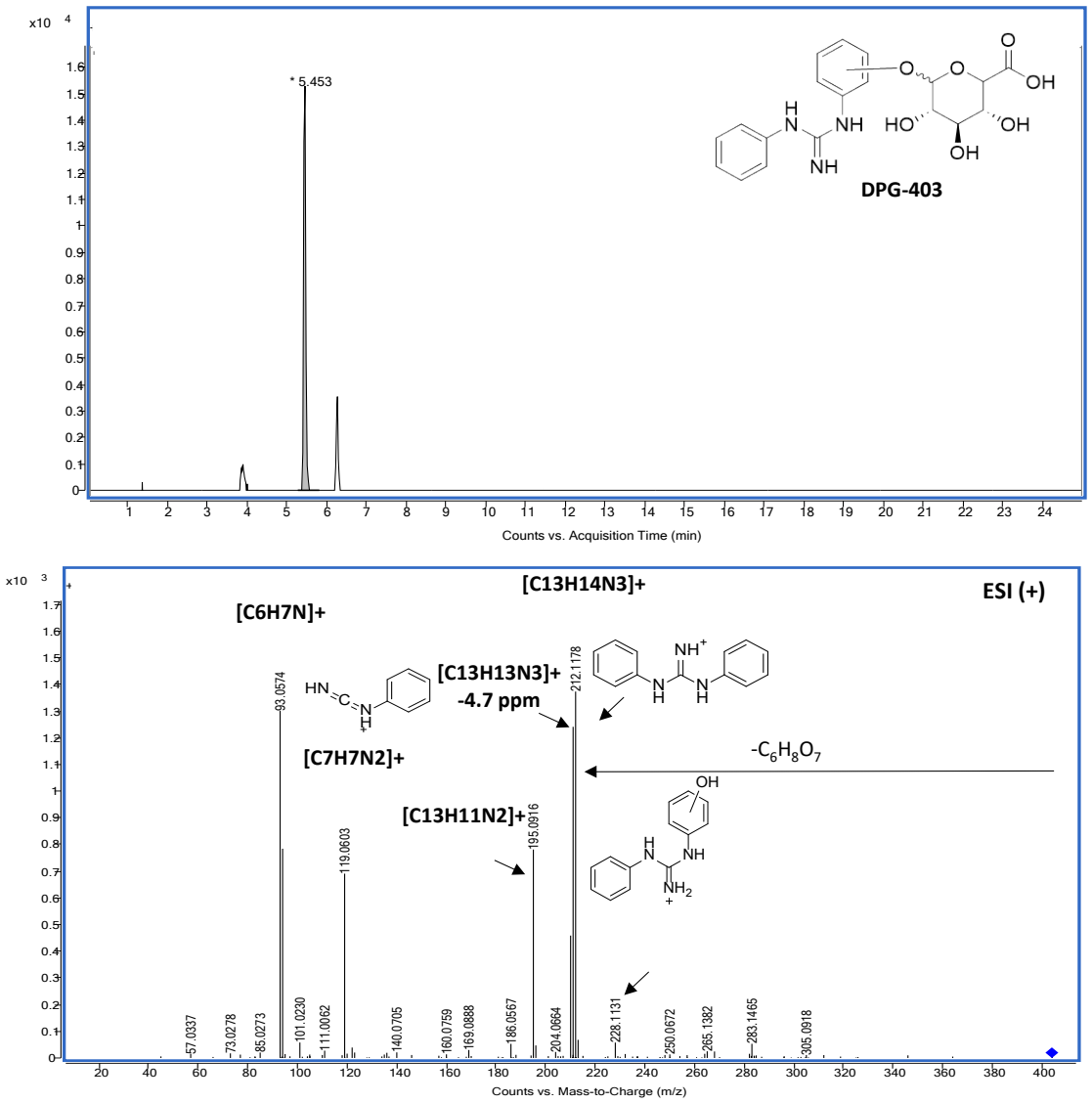

Figure S14. Extracted ion chromatogram and MS/MS spectrum at 20 V with proposed fragmentation pattern for DTG-415.

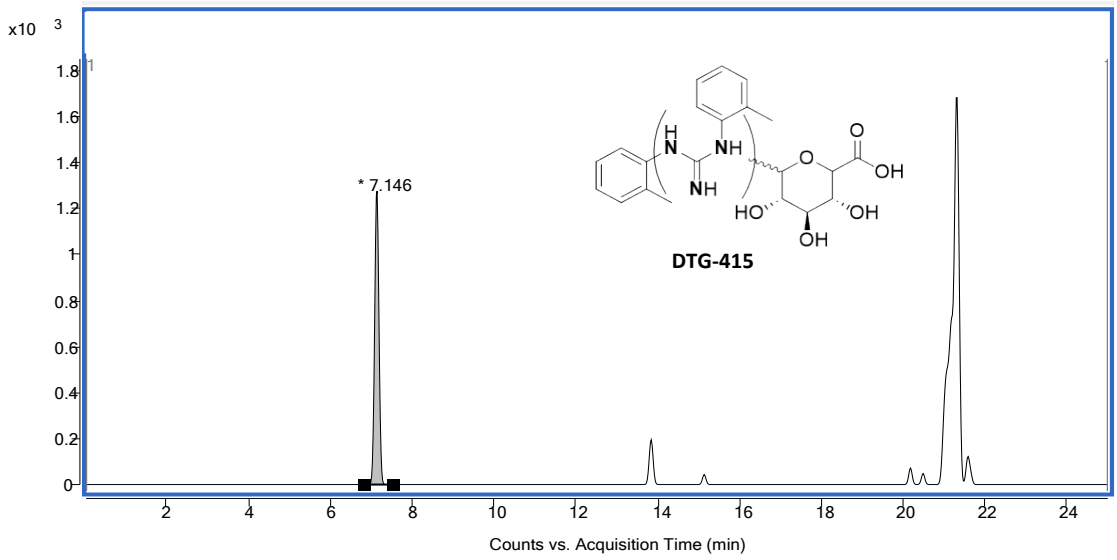

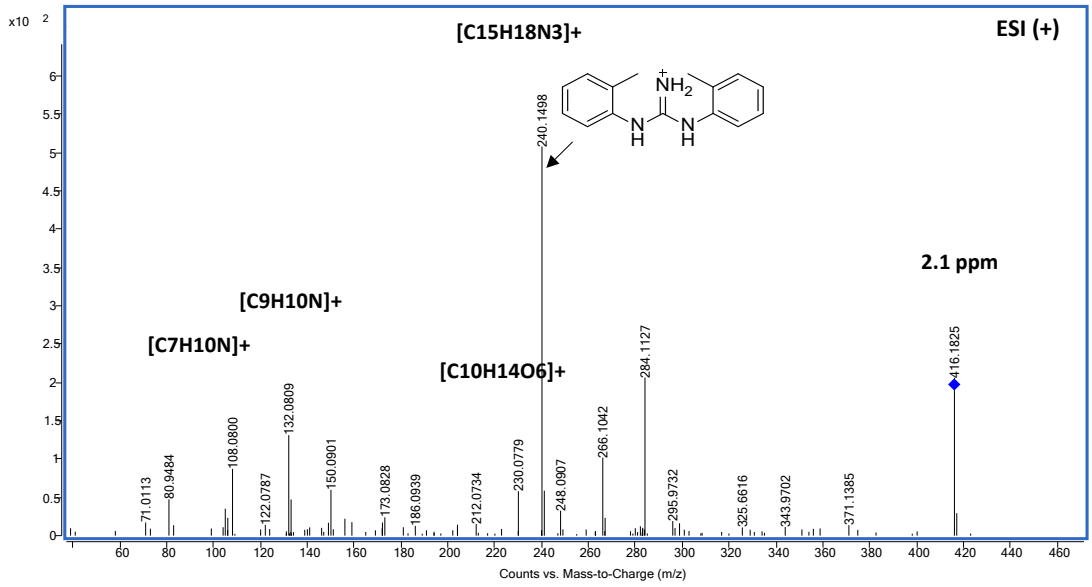

Table S4. Urinary levels of DPG, DPG-227 and DTG and, MS/MS transition ratios of identified target chemicals in pooled samples.

	DPG			DPG-227			DPG-387		DPG-403		DTG		
	Concentration µg L^{-1}	Q_2/Q_1	Q_3/Q_1	Concentration [b] µg L^{-1}	Q_2/Q_1	Q_3/Q_1	Q_2/Q_1	Q_3/Q_1	Q_2/Q_1	Q_3/Q_1	Concentration µg L^{-1}	Q_2/Q_1	Q_3/Q_1
P1	0.119	1.2	0.50	0.092	0.76	0.30	Only Q_1 [a]	Only Q_1 [a]	Only Q_1 [a]	Only Q_1 [a]	0.063	0.90	0.36
P2	0.083	1.2	0.52	0.035	0.87	0.32	Only Q_1 [a]	Only Q_1 [a]	Only Q_1 [a]	Only Q_1 [a]	0.058	1.0	0.41
P3	0.043	1.3	0.52	0.043	1.0	0.30	Only Q_1 [a]	Only Q_1 [a]	Only Q_1 [a]	Only Q_1 [a]	0.056	0.91	0.34
P4	0.040	1.3	0.54	0.025	1.0	0.32	Only Q_1 [a]	Only Q_1 [a]	Only Q_1 [a]	Only Q_1 [a]	0.024	0.93	0.36
P1d[c]	0.227	1.4	0.54	0.101	0.65	0.31	Not detected	Not detected	Not detected	Not detected	0.209	1.0	0.37
P2d[c]	0.188	1.3	0.81	0.049	1.0	0.29	Not detected	Not detected	Not detected	Not detected	0.060	1.0	0.40
P3d[c]	0.073	1.3	0.78	0.073	0.65	0.19	Not detected	Not detected	Not detected	Not detected	0.115	1.0	0.46
P4d[c]	0.090	1.1	0.65	0.045	0.84	0.25	Not detected	Not detected	Not detected	Not detected	0.071	1.1	0.39

[a] Only one MS/MS transition was identified.

[b] DPG-227 concentration was calculated assuming a response equal to that of DPG, from its standard addition calibration curve.

[c] Deconjugated set of urine samples.

Figure S15. Chromatographic peaks of MS/MS transitions for DPG-387 and DPG-403 found in HLM (left) and urine (right) samples.